THE JOURNAL OF PHYSICAL CHEMISTRY LETTERS
A JOURNAL OF THE AMERICAN CHEMICAL SOCIETY

pubs.acs.org/JPCL

Letter

Probing Through-Bond and Through-Space Interactions in Singlet Fission-Based Pentacene Dimers

Ashish Sharma, Stavros Athanasopoulos, Yun Li, Samuel N. Sanders, Elango Kumarasamy, Luis M. Campos, and Girish Lakhwani*

Cite This: J. Phys. Chem. Lett. 2022, 13, 8978−8986

Read Online

ACCESS | Metrics & More | Article Recommendations | Supporting Information

ABSTRACT: Interchromophoric interactions such as Coulombic coupling and exchange interactions are crucial to the functional properties of numerous π-conjugated systems. Here, we use magnetic circular dichroism (MCD) spectroscopy to investigate interchromophoric interactions in singlet fission relevant pentacene dimers. Using a simple analytical model, we outline a general relationship between the geometry of pentacene dimers and their calculated MCD response. We analyze experimental MCD spectra of different covalently bridged pentacene dimers to reveal how the molecular structure of the "bridge" affects the magnitude of through-space Coulombic and through-bond exchange interactions in the system. Our results show that through-bond interactions are significant in dimers with conjugated molecules as bridging units and these interactions promote the overall electronic coupling in the system. Our generalized approach paves the way for the application of MCD in investigating interchromophoric interactions across a range of π-conjugated systems.

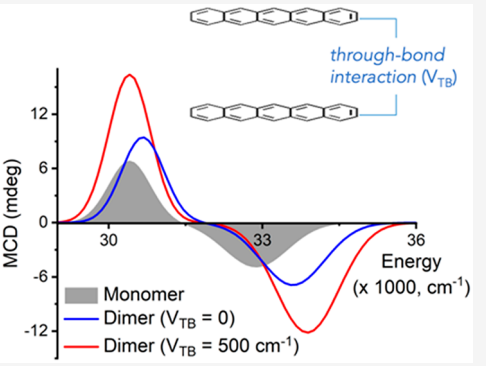

π-Conjugated systems offer great promise as photoactive layer materials in optoelectronic devices, such as photovoltaics,[1] light-emitting diodes,[2] photodetectors,[3] and bioelectronics.[4] The development of efficient organic electronic devices is dependent on a fundamental understanding of the interchromophoric interactions that affect the absorption of light and subsequent energy relaxation in conjugated systems. These interactions can be conveniently categorized as through-space Coulombic interactions between resonant molecular dipoles and through-bond exchange interactions between molecules with a significant wave function overlap.[5,6] The latter is especially important in the case of thin films with closely packed molecules as well as covalently bridged systems, such as dimers and oligomers, where the "bridging unit" can promote indirect overlap between the chromophores.[7,8] Insights into the magnitudes of through-space and through-bond interactions are crucial for understanding the relationship between intermolecular coupling and photophysical processes such as energy and charge transfer, key to developing rational design criteria for improved functional materials.

An example system in which interchromophoric interactions significantly affect electronic transitions as well as energy and charge transfer is the family of pentacene dimers. Specifically, pentacene dimers with strongly interacting monomer units undergo intramolecular singlet exciton fission (SF), a process through which the photoexcited spin-0 singlet state converts to a pair of spin-1 triplet states.[9] Because of the potential of SF to enhance the performance of organic and hybrid solar cells,[10,11] considerable effort has been spent to develop structure−property insights into SF dynamics and to design efficient SF-based materials.[12−15] In this regard, covalently bridged pentacene dimers have been widely investigated as the molecular structure of the bridge allows a handle to tailor the inter-pentacene interactions and, subsequently, the SF dynamics.[16−23] While it is anticipated that bridge-mediated through-bond interactions are crucial to SF dynamics, investigations into the extent of these interactions have been limited.

We have recently shown that optical activity, i.e., the differential interaction of left- and right-circularly polarized light (CPL) with chiral molecules, can sensitively probe bridge-mediated through-bond interactions in an axially chiral binaphthyl pentacene dimer.[24] Our results demonstrated that ground and excited state circular dichroism (CD) spectroscopic measurements of optical activity can prove to be useful in investigating the complex nature of pentacene−bridge interactions that underpin SF dynamics and subsequently assist in the design of next-generation SF molecular systems. Magnetic circular dichroism (MCD) spectroscopy is another optical technique that can be used to measure induced optical activity in chromophores under the influence of an applied magnetic field; however, this method does not require that molecular systems

Received: July 2, 2022
Accepted: September 15, 2022
Published: September 23, 2022

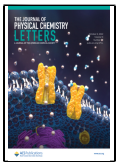

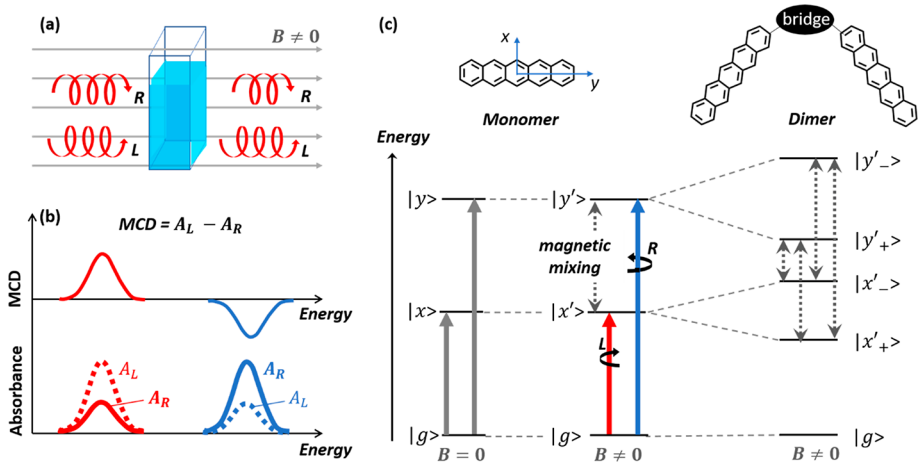

Figure 1. Schematic of the MCD measurement and the relevant energy diagrams. (a) Schematic of a solution MCD measurement that shows attenuated differential transmission of left (L) and right (R) circularly polarized light in the presence of a magnetic field, B, in a Faraday geometry. (b) B-Type MCD spectra that originate from the preferential absorption, A_L and A_R of L and R circularly polarized light, respectively. (c) Schematic energy diagrams of a pentacene monomer and a dimer. Under an applied magnetic field, magnetic mixing (shown as a gray dashed double-headed arrow) between monomeric states $|x\rangle$ and $|y\rangle$ perturbs the wave functions such that $|x'\rangle = |x\rangle + i\delta(B)|y\rangle$ and $|y'\rangle = |y\rangle + i\delta(B)|x\rangle$. In the case of a dimer, excitonic coupling between the monomeric states can give rise to new so-called "in phase" and "out of phase" coupled excited states, $|x'_+\rangle$, $|y'_+\rangle$ and $|x'_-\rangle$, $|y'_-\rangle$, respectively, that can undergo further magnetic mixing resulting in a markedly different MCD spectrum.

be chiral.[25,26] Specifically, the MCD response, measured as the differential absorption of left- and right-handed CPL in the presence of an applied magnetic field in a Faraday geometry (Figure 1), has been used to investigate the electronic structure of quantum dots,[27] nanoplatelets,[28] metallocomplexes,[29] and numerous π-conjugated systems.[30−32] The sign and shape of the MCD spectra of numerous cyclic π-conjugated systems such as naphthalenes,[33] acenes,[34] phenylenes,[35] porphyrins,[25,36] thioimides,[37] and other compounds[38] have been studied to understand the role of electronic structure, i.e., the effect of electron-donating or -withdrawing substituents, dimerization, and aggregation on their magneto-optical electronic properties. Notably, the analysis of the strength of the MCD response has provided detailed insights into the internal aggregate structure of chlorophyll molecules[38−40] and several other conjugated systems.[25,41] A well-developed theoretical framework, such as Michl's perimeter model, is often used for the qualitative analysis of the MCD spectra.[42] Furthermore, in comparison to CD, MCD is much more sensitive to local perturbations in molecular structure and has been used to separate local intermolecular interactions from long-range dipolar coupling in molecular aggregates.[41,43] In the case of SF-based pentacene dimers, local bridge-mediated through-bond interactions and through-space dipolar interactions crucially affect the SF process.[17,19,44] In this vein, MCD can be exploited to selectively identify the extent of bridge-mediated interactions in SF-based systems; however, this has hitherto never been investigated.

In this report, we use the MCD spectral signatures of the 6,13-bis(triisopropylsilylethynyl) pentacene (TIPS-Pc) monomer and various covalently bridged pentacene dimers to investigate intramolecular interactions between two pentacene chromophores. Figure 1 shows the schematic of the MCD experiment and the energy diagrams highlighting the effect of excitonic coupling on the observed MCD response. Using density functional theory (DFT) calculations and Gaussian analysis of the MCD bands, we first qualitatively explain the origins of the MCD spectra of TIPS-Pc. We advance existing theoretical models to extract the magnitude of through-space and through-bond interactions from the MCD spectra of different covalently bridged pentacene dimers. Our results suggest that through-bond interactions are significant in dimers with π-conjugated bridging units, suggesting that these interactions are predominantly of the "resonance" type. These results are consistent with the McConell model,[45] which suggests that significant through-bond interactions in covalently bridged dimers necessitate delocalization of the electronic density on the bridging unit. Comparing the reported SF dynamics in the literature of the covalently bridged dimers studied here with the extent of overall electronic coupling in the system determined by our MCD measurements, we hypothesize that resonance-type through-bond interactions are beneficial to the SF process. Our approach highlights the promising role of MCD spectroscopy as a simple, sensitive tool for investigating the through-space and through-bond interactions in conjugated systems, especially relevant for SF-based materials.

We first discuss the ground state absorption spectrum of dilute solutions of the TIPS-Pc monomer in Figure 2a. Three distinct features can be easily identified from the electronic absorption spectrum of TIPS-Pc: an intense peak in the high-energy region around 320 nm, a moderately intense absorption band with characteristic vibrational progression in the low-energy region around 650 nm, and a very weak absorption band in the region around 400 nm. These absorption signatures are characteristic of acenes, and their origins have been discussed previously.[46−48] Briefly, the lowest-energy absorption band is attributed to the "p" transition, which results from an excitation into a ^1L_a state of B_{2u} symmetry and is polarized along the short axis of the pentacene molecule. The weak absorption peak around 400 nm and an intense peak at 320 nm are suggested to arise from photoexcitation from the ground state to excited states ^1L_b (α transition) and ^1B_b (β transition), respectively, and are polarized along the long molecular axis. An additional peak to the red of the β band, observed here at 340 nm, has been previously assigned to excitation to $2^1B_{3u}^-$ and $2^1B_{2u}^+$ states (labeled as the "x" transition to the 2^1L_a state in Figure 2c).

https://doi.org/10.1021/acs.jpclett.2c02061
J. Phys. Chem. Lett. 2022, 13, 8978−8986

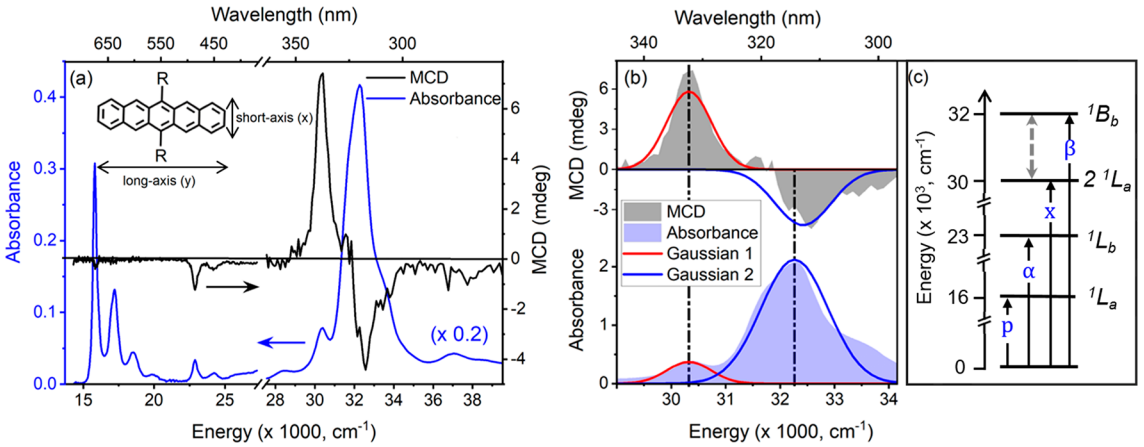

Figure 2. MCD and absorbance of the monomer TIPS-Pc. (a) Absorbance (blue lines) and MCD (black lines) of a 3 μM solution of the 6,13-bis(triisopropylsilylethynyl) pentacene (TIPS-Pc) monomer in dichloromethane. The inset of panel a shows the molecular structure of TIPS-Pc, where R = a triisopropylsilylethynyl (TIPS) group with arrows depicting the long- and short-axis polarized transitions. (b) Gaussian fits (red and blue lines) to the MCD and absorbance of high-energy transitions of TIPS-Pc overlaid on the significant bisignate B-type MCD response (shaded gray region) and absorption spectrum (shaded blue region) of TIPS-Pc. The dashed−dotted lines in panel b highlight that peaks in MCD and absorption spectra align very well, as expected from B-type MCD. (c) Energy diagram of TIPS-Pc depicting the electronic transitions and the energies of the relevant excited states. Magnetic mixing between the high-energy states is highlighted by the dashed gray double arrow.

The MCD spectrum of TIPS-Pc has positive and negative lobes whose peaks align with absorption peaks at 340 and 320 nm, respectively, as shown in Figure 2b, suggesting that the origin of MCD in TIPS-Pc is purely B-type.[30] B-Type MCD is commonly observed in molecules that lack C_3 (or higher) symmetry in the molecular structure. The sign and transition energy of the lobes observed in the MCD spectrum of TIPS-Pc agrees well with the predicted values from Michl's model, confirming that the B-type MCD predominantly originates from magnetic field-induced mixing between the L and B excited states.[31] This is further established by our quadratic response density functional theory (QR-DFT) calculations, which can qualitatively reproduce the MCD spectrum assuming first-order excited state mixing as the origin of the MCD response (Tables S1 and S2 and Note S1).

Experimentally, the strength of the MCD response, i.e., the magnitude of the B term for a given transition, can be calculated using the area under the measured MCD lobe.[38] The strength of the MCD response is often discussed in terms of the B/D ratio that is defined as the ratio of the magnitude of the B term to dipolar strength D of a transition and can be calculated using eqs 1 and 2.

$$\text{MCD (mdegs)} = 32982 * \Delta A \tag{1}$$

$$\frac{B}{D} = \frac{0.714 \int \Delta A \, d\upsilon}{\int A \, d\upsilon} \tag{2}$$

where ΔA $(= A_L - A_R)$ refers to the difference in the absorption L (A_L) and R (A_R) circularly polarized light of a transition under an applied magnetic field in Faraday geometry, υ represents the energy in units of inverse centimeters, and A refers to the absorption of a given transition. Upon approximation of individual transitions as Gaussian-shaped, the B/D value of each TIPS-Pc MCD lobe can be calculated by simultaneously fitting Gaussian bands to the experimental absorption and MCD spectra, as shown in Figure 2b. For TIPS-Pc, the B/D value is calculated as 0.5×10^{-4} cm^{-1} (β transition at 320 nm), which is on the same order of magnitude as reported B/D values of other organic systems such as porphyrins,[25] perylenes,[41] and acenes.[49]

Theoretically, the magnitude and sign of a B-type MCD response can be estimated by calculating the B terms of individual transitions. The B term of a transition from ground state $|g\rangle$ to a particular excited state $|i\rangle$ is given by the field-induced mixing of state $|i\rangle$ with the other excited states, as expressed in eq 3.[32]

$$B_i = Im \sum_{j \neq i} \frac{m_{ij}(\mu_i \times \mu_j)}{\Delta E_{ij}} \tag{3}$$

where m_{ij} represents the magnetic transition dipole moment between $|i\rangle$ and another excited state $|j\rangle$, μ_i and μ_j represent the electronic transition dipole moments of the transitions from ground state $|g\rangle$ to states $|i\rangle$ and $|j\rangle$, respectively, and ΔE_{ij} is the difference between the energy of states $|i\rangle$ and $|j\rangle$. The cross product in eq 3 implies that MCD for a given transition is predominantly influenced by other orthogonally polarized transitions. Thus, in the case of TIPS-Pc, significant MCD can be expected in regions where short-axis and long-axis polarized transitions are close in energy. Furthermore, bisignate-shaped MCD should be obtained if the magnetic field mixing primarily involves only two excited states.

We attribute the bisignate-shaped MCD feature in the high-energy region of TIPS-Pc primarily to magnetic field-induced mixing between 2^1L_a and ^1B_b states (Figure 2c). Using eq 3, we obtain a lower bound value of 0.9 Bohr magneton for the magnetic transition dipole moment between these states. This is comparable to the reported values for the magnetic transition dipole moment between excited states of porphyrins[25] and other cyclic acenes,[41,49] suggesting that the MCD in TIPS-Pc and porphyrins shares a similar origin, i.e., arising from the nature of the molecular orbitals involved. In summary, TIPS-Pc shows a bisignate-shaped B-type MCD, especially in the high-energy region, that can be attributed to magnetic field-induced mixing between two close-lying excited states with orthogonal symmetry.

https://doi.org/10.1021/acs.jpclett.2c02061
J. Phys. Chem. Lett. 2022, 13, 8978−8986

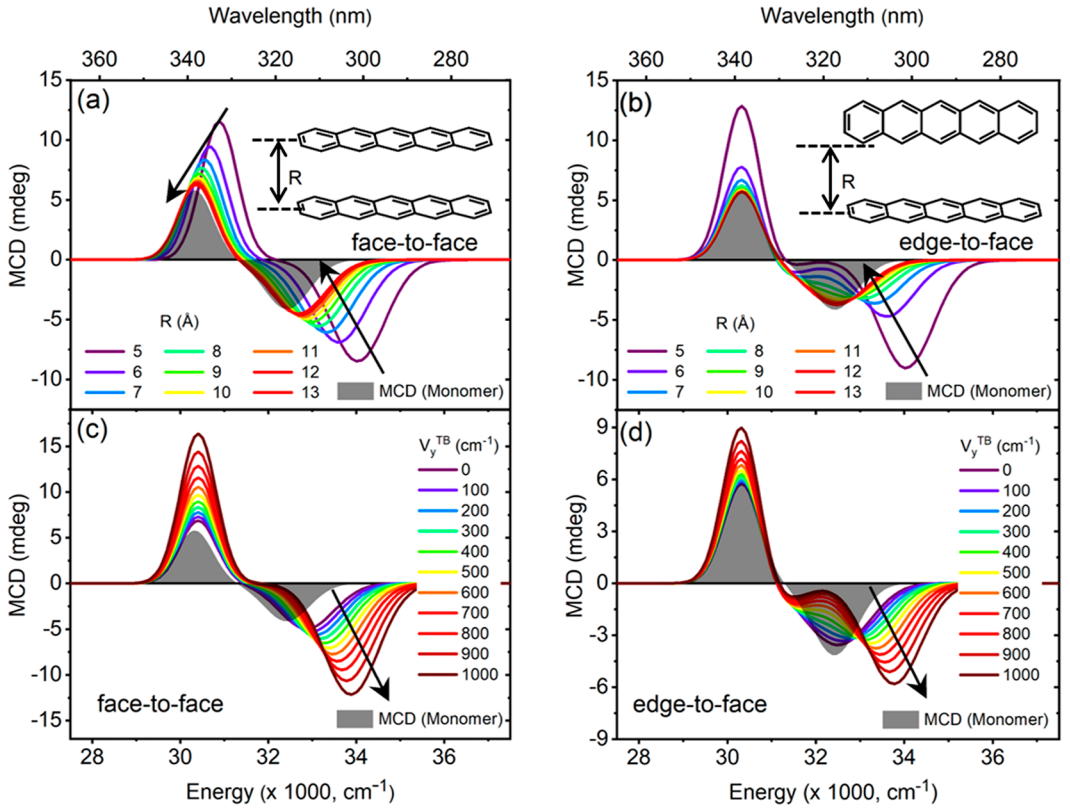

Figure 3. Effect of through-space and through-bond interactions on the MCD of pentacene dimers. Calculated MCD of a pentacene dimer with only through-space dipolar coupling ($V_y^{TB} = 0$) included for (a) the face-to-face configuration and (b) the edge-to-face configuration. Insets of panels a and b show the face-to-face and edge-to-face configurations, respectively, where R is the inter-pentacene distance. Calculated MCD of a pentacene dimer for $R = 1$ nm for (c) the face-to-face configuration and (d) the edge-to-face configuration varying the magnitude of through-bond interaction potential (V_y^{TB}) between long-axis polarized transitions of the pentacene units.

To identify whether MCD can be exploited as a spectroscopic marker of inter-pentacene interactions, we calculate the MCD spectra of a pentacene dimer by varying the magnitude of through-space and through-bond interactions between pentacene chromophores. For the former, we calculate the MCD spectra of different pentacene dimers by systematically varying the distance between the two pentacene chromophores in the dimer geometry (Figure 3a,b and Figure S3). Here, the magnitude of through-space interaction for a given geometry is obtained by calculating the dipolar coupling between monomer pentacene transitions using a line-dipole approximation, with the magnitudes of coupling further confirmed using TD-DFT calculations (see Note S2 and Figures S1 and S2).

Panels a and b of Figure 3 show the exclusive impact of through-space dipolar coupling on the bisignate MCD spectrum in the region of 28000−40000 cm^{-1} as two pentacene units are brought closer to each other with a defined relative orientation. We consider two relevant configurations, face-to-face and edge-to-face, that have been observed in pentacene aggregates, thin films, and crystals.[50] While the face-to-face configuration represents the geometry where inter-pentacene coupling between both short- and long-axis transitions can be maximized, the edge-to-face configuration models a pentacene dimer system with orthogonal pentacene units. Here, through-space dipolar coupling of monomers results in the splitting of a monomeric transition into a high-energy "out-of-phase" transition and a low-energy "in-phase" transition (as shown in Figure 1c). The effect of through-space dipolar coupling on the MCD response dimers can be determined by calculating the magnetic transition dipole moment between the dimer excited states (see Note S2, Figure S3 and Table S4). For instance, if excitonic coupling between the long-axis polarized transitions from the ground state to an excited state $|y\rangle$ results in an "in-phase" transition to $|y_+\rangle$ and an "out-of-phase" transition to $|y_-\rangle$, the B terms for these new transitions can be calculated using eqs 4−6.

$$B_{y_+} = -\frac{1}{4}(m_{xy}\mu_x\mu_y)\left(\frac{1 + R_{11} + R_{22} + R_{33}}{E_{x_+} - E_{y_+}} + \frac{1 - R_{11} - R_{22} + R_{33}}{E_{x_-} - E_{y_+}}\right) \quad (4)$$

$$B_{y_-} = -\frac{1}{4}(m_{xy}\mu_x\mu_y)\left(\frac{1 - R_{11} + R_{22} - R_{33}}{E_{x_+} - E_{y_-}} + \frac{1 + R_{11} - R_{22} - R_{33}}{E_{x_-} - E_{y_-}}\right) \quad (5)$$

$$E_{i_\pm} = E_i \mp V_i^{TS} \quad (i = x, y) \quad (6)$$

where m_{xy} represents the magnetic transition dipole moment between $|y\rangle$ and another excited state $|x\rangle$, μ_x and μ_y represent the

https://doi.org/10.1021/acs.jpclett.2c02061
J. Phys. Chem. Lett. 2022, 13, 8978−8986

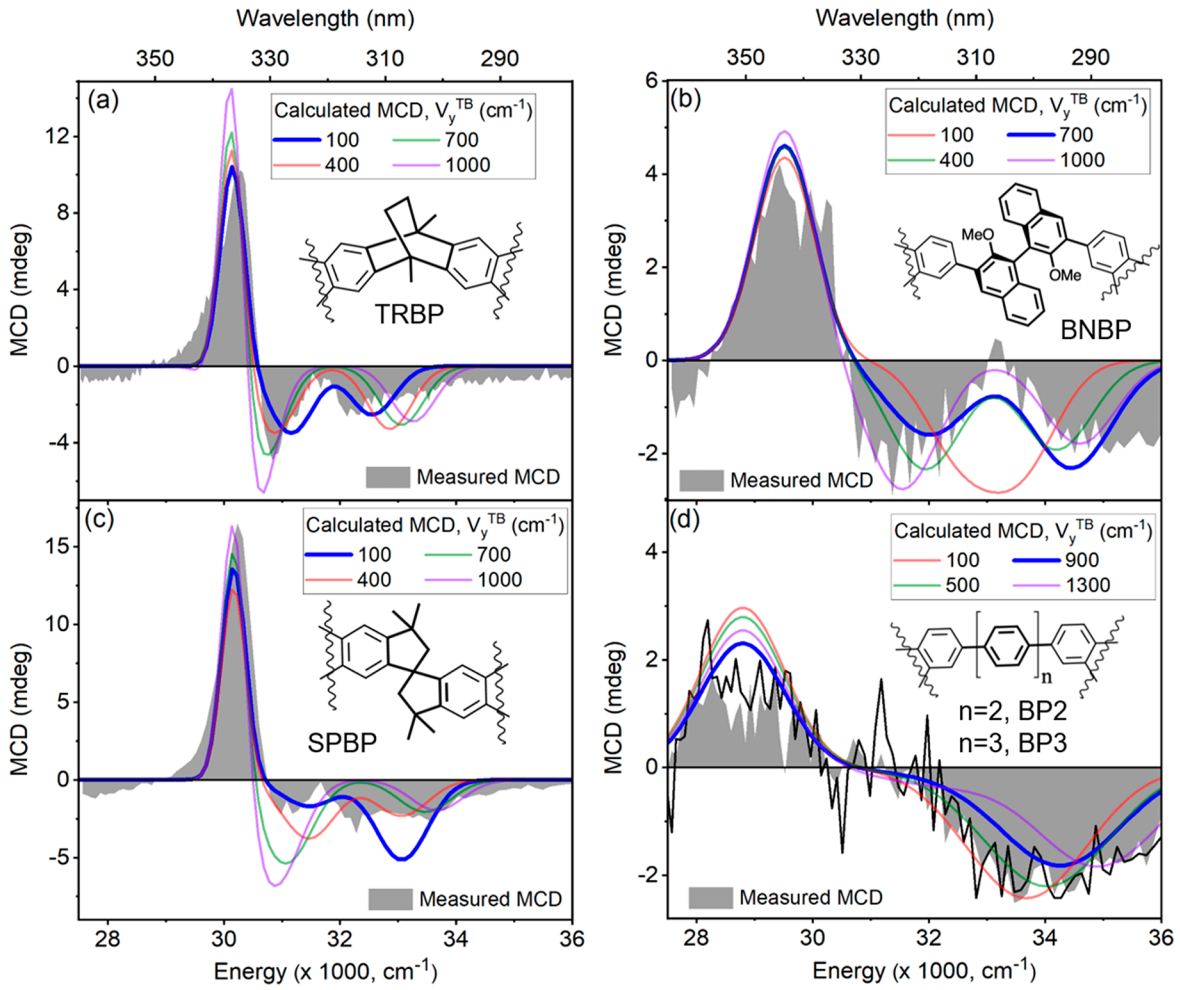

Figure 4. MCD of covalently linked pentacene dimers. Experimental (shaded regions) and calculated (colored lines) MCD for 3 μM solutions of pentacene dimers (a) TRBP, (b) SPBP, (c) BNBP, and (d) BP2 and BP3 in dichloromethane. The calculated spectrum (blue) best fits the experiment for each pentacene dimer. The insets show the molecular structures of the dimers.

electronic transition dipole moment of the "monomeric" transitions from ground state $|g\rangle$ to states $|x\rangle$ and $|y\rangle$ that are polarized along the short axis and long axis of the pentacene unit, respectively, R_{11}, R_{22}, and R_{33} refer to the (1, 1), (2, 2), and (3, 3) elements, respectively, of the Euler rotation matrix used to relate the molecular coordinate axis of the individual monomers in the dimer geometry (see Note S2), E_i, E_{i_+}, and E_{i_-} $(i = x, y)$ are the energies of the "monomeric" transition, the "out-of-phase" and "in-phase" excitonically coupled short-axis $(i = x)$ and long-axis $(i = y)$ polarized transitions in the dimer geometry, respectively, and V_i^{TS} represents the through-space dipolar coupling between pentacene units for short-axis $(i = x)$ and long-axis $(i = y)$ polarized transitions. Similar equations can be obtained for calculating the B terms of "short-axis" polarized transitions to obtain the MCD spectra of the dimer configurations (see Note S2). Although, through-space dipolar coupling can also contribute to the observed MCD through induced orbital angular momentum in the excited states, these contributions are usually too small to be relevant for most organic systems and have been ignored here.[51]

As one can see in panels a and b of Figure 3, for large inter-pentacene separation, MCD spectra of monomer and dimer configurations are similar. With a decrease in the inter-pentacene separation, the through-space dipolar coupling between the pentacene units increases, resulting in changes to the MCD spectra. These changes in the MCD response are sensitive to the relative orientation of the pentacene units. For a dimer configuration in which pentacene units are held face-to-face, an increase in dipolar coupling results in a blue-shift and a concomitant increase in the magnitude of the bisignate MCD response. On the contrary, for pentacenes arranged in an "edge-to-face" configuration, an increase in dipolar coupling predominantly affects the shape of the higher-energy negative lobe. This is expected as the through-space dipolar coupling between the orthogonal short-axis transitions in the "edge-to-face" configurations is reduced.

More generally, the effect of through-space dipolar coupling on the MCD response for different configurations of pentacene dimers and other oligomers can be calculated (see Note S3 and Figure S4). Comparing MCD spectra for different dimer geometries, we estimate that the minimum value of V_y^{TS} required for an observable change in the shape and/or magnitude of the MCD response is ~500 cm^{-1}. This implies that for a transition with a dipolar strength of 1 D, an inter-pentacene separation of <1 nm is required for the MCD spectra of this transition to be affected by through-space dipolar coupling in the dimer.

https://doi.org/10.1021/acs.jpclett.2c02061
J. Phys. Chem. Lett. 2022, 13, 8978−8986

For pentacene dimers with covalently linked bridging units, bridge-mediated through-bond interactions can be significant. The through-bond interactions are usually approximated as a through-bond interaction potential (V^{TB}) that contributes to the total electronic coupling in the system.[52] Notably, very large values of V^{TB} ($\lesssim$3000 cm^{-1}) have been reported for the strongly allowed β transitions in covalently bridged anthracene dimers.[6] To investigate whether through-bond interaction of the β transition in pentacene dimers can influence the MCD spectrum, we calculated the MCD spectra of pentacene dimers by including a through-bond interaction potential (V_y^{TB}) that contributes to the total electronic coupling (V_y) of the β transition in the system (eq 7).

$$E_{y_\pm} = E_y \mp (V_y^{TS} + V_y^{TB}) \tag{7}$$

While non-zero V_i^{TS} ($i = x, y$) can be obtained for any pentacene dimer configuration, V_y^{TB} can have non-zero values only in covalently bridged pentacene dimers with significant through-bond interaction of the high-energy β transition. Panels c and d of Figure 3 show that even for a small value of V_y^{TB} the MCD spectrum changes appreciably. For instance, inclusion of V_y^{TB} in the "face-to-face" dimer configuration results in an increase in the MCD magnitude and a small blue-shift in the high-energy lobe. For the "edge-to-face" dimer configurations, an increase in V_y^{TB} results in a remarkable splitting of the negative MCD lobe at ~32000 cm^{-1}. These complementary and distinct changes observed in the calculated MCD spectrum emphasize its sensitivity and usefulness in differentiating through-space and through-bond interactions in pentacene dimers.

We now compare experimental MCD spectra for different covalently bridged pentacene dimers with the calculated MCD spectra to investigate the extent of through-space and through-bond interactions in these systems. The molecular structures of the bridging units in these dimers are shown in the inset of Figure 4. While the "bridging units" in TRBP and SPBP have nonconjugated bonds, BNBP, BP2, and BP3 involve bridging units with conjugated benzene rings.

Akin to their TIPS-Pc monomer, dilute solutions of all of the covalently bridged pentacene dimers show appreciable B-type MCD spectra as shown in Figures 2 and 4 (for the complete spectral range, see Figures S4−S8). The shape of the MCD spectra of the dimers is markedly different from the that of the MCD spectra of TIPS-Pc, especially the negative lobe in the high-energy region. While a splitting of the negative MCD lobe is observed for dimers with homoconjugated bridges (TRBP, SPBP, and BNBP), dimers with conjugated bridges (BP2 and BP3) exhibit a broadened and blue-shifted negative MCD lobe. Although not as clearly, such spectral changes can also be concomitantly observed in the absorption spectra of the dimers in the region of 31000−35000 cm^{-1} (see Figures S5−S12).

Next, using the DFT-optimized geometries, we calculate the MCD spectra for all dimers. Here, parameters such as the energies and widths of the transitions are independently inferred from the absorption spectra of the dimer and the through-space dipolar coupling between the transitions is defined by the dimer geometry. We note that the values of through-space excitonic coupling between the long-axis polarized transitions (V_y^{TS}) used to fit the MCD spectra of pentacene dimers agree very well with the calculated values of V_y^{TS} at the TD-DFT level with CAM-B3LYP/6-31G(d,p)-optimized molecular geometries (Table S3). The only other variable parameter used to fit the MCD spectra is the through-bond interaction potential (V_y^{TB}) between the β transitions. As expected, the magnitude of V_y^{TB} affects the shape and strength of the MCD response of the dimers. In the case of dimers TRBP, SPBP, and BNBP with an almost orthogonal relative orientation of pentacene units, an increase in V_y^{TB} is associated with a change in the shape and energies of the split negative MCD lobes (Figure S12). For dimers BP2 and BP3 with a collinear arrangement of pentacenes, an increase in V_y^{TB} results in an increase in the separation between the positive and negative MCD lobes (Figure S12). As shown in Figure 4, we can satisfactorily reproduce the measured MCD spectra of different dimers to reveal how V_y^{TB} varies across the different covalently bridged pentacene dimers.

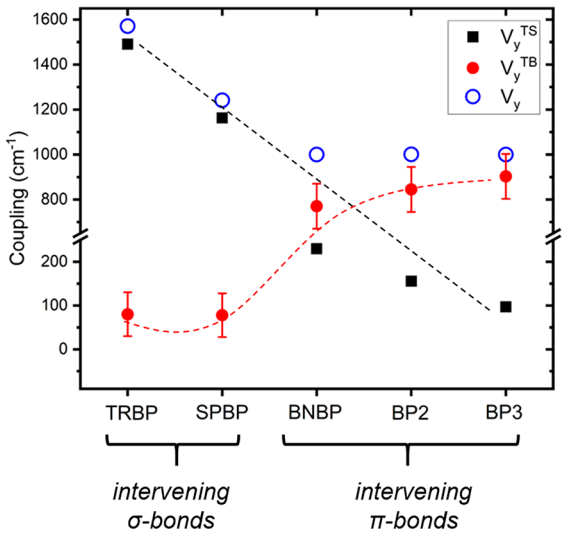

Figure 5. Through-space and through-bond coupling in pentacene dimers. Magnitude of through-space coupling (V_y^{TS}), though-bond coupling (V_y^{TB}), and total coupling (V_y) between the long-axis polarized monomeric β transitions in different pentacene dimers obtained by fitting the experimental MCD spectrum. The black and red dashed lines are guides to the eye. The error bars in V_y^{TB} are determined by comparing the calculated and experimental MCD spectra.

In Figure 5, we discuss the effect of the bridging unit on the magnitudes of through-space coupling (V_y^{TS}), though-bond coupling (V_y^{TB}), and total coupling ($V_y = V_y^{TS} + V_y^{TB}$) between the monomeric "β" transitions across the different pentacene dimers. As expected, V_y^{TS} decreases with an increase in the size of the "bridging unit". For instance, while magnitudes of V_y^{TS} > 1000 cm^{-1} are obtained for dimers TRBP and SPBP, the magnitude of V_y^{TS} is at least 5 times lower for dimers BNBP, BP2, and BP3, primarily a result of the larger inter-pentacene separation in the latter. Interestingly, V_y^{TB} follows an almost reverse trend in comparison to V_y^{TS} for these systems. While the

https://doi.org/10.1021/acs.jpclett.2c02061
J. Phys. Chem. Lett. 2022, 13, 8978−8986

dimers incorporating conjugated bridges (BP2 and BP3) exhibit high magnitudes of V_y^{TB} ($\lesssim$1000 cm^{-1}), V_y^{TB} is almost insignificant in dimers TRBP and SPBP that involve bridging units constituted by σ bonds. Furthermore, an intermediate value of V_y^{TB} (~700−800 cm^{-1}) is obtained for dimer BNBP that incorporates a homoconjugated "binaphthyl" bridge, consistent with the value of through-bond coupling estimated through circular dichroism measurements of BNBP previously.[24] The observed dependency of V_y^{TB} on the conjugation in the bridging unit suggests that through-bond interactions in covalently bridged pentacene dimers are of the "resonance type", mediated by a pathway involving the intervening bonds of the spacer. It can thus be anticipated that the key parameter controlling the through-bond coupling in these systems is the delocalization of electronic density on the bridging units, as also predicted from the McConnell model on the through-bond interactions in covalently bridged acene-based systems.[45]

We have previously shown that these dimer molecules can undergo SF in dilute solutions and that the bridging unit modulates the rates of SF in these systems.[17,23,24] For instance, triplet−triplet annihilation (TTA) via an intermediate triplet pair (TT) state has been found to be a predominant decay pathway in dimers TRBP and SPBP,[17] while it is significantly suppressed in the case of dimers BP2 and BP3[23] and almost completely suppressed in the case of BNBP.[24] These variations in the TTA cannot be simply explained by the magnitude of through-space dipolar coupling of the pentacene units in these systems.[14,44] We infer that the magnitude of through-bond coupling, V_y^{TB}, is correlated with the rate of TTA in these dimers. Specifically, for dimers BNBP, BP2, and BP3 in which inter-pentacene coupling is predominantly controlled by through-bond interactions, the triplet−triplet annihilation pathway is suppressed. It is likely that through-bond interactions in these systems significantly affect the TTA dynamics,[44,53,54] and further study is required to confirm this hypothesis. Excited state MCD measurements of covalently bridged pentacene dimers could be an interesting direction for future work in unraveling the complex role of bridge-mediated through-bond interactions in the TTA dynamics and in turn the SF dynamics.

In conclusion, we have shown that MCD can be used as a sensitive spectroscopic method for probing through-space and through-bond interactions in covalently bridged pentacene dimers. We demonstrate that through-bond interactions are dominant in pentacene dimers involving conjugated molecules as bridging molecules. These results are useful in understanding the role of the bridging units in the observed SF dynamics of these systems. We anticipate that our approach can be extended more generally to investigate through-bond and through-space coupling across a range of π-conjugated systems.

■ ASSOCIATED CONTENT

Supporting Information

The Supporting Information is available free of charge at https://pubs.acs.org/doi/10.1021/acs.jpclett.2c02061.

Details of the experimental procedures, the model for calculating the MCD response of dimers, MCD measurements at different concentrations, and details of the theoretical and computational analysis (PDF)

■ AUTHOR INFORMATION

Corresponding Author

Girish Lakhwani − *ARC Centre of Excellence in Exciton Science, School of Chemistry, The University of Sydney, Sydney, New South Wales 2006, Australia; The University of Sydney Nano Institute, Sydney, New South Wales 2006, Australia;* orcid.org/0000-0003-1070-5859; Email: girish.lakhwani@sydney.edu.au

Authors

Ashish Sharma − *ARC Centre of Excellence in Exciton Science, School of Chemistry, The University of Sydney, Sydney, New South Wales 2006, Australia; Cavendish Laboratory, University of Cambridge, Cambridge CB3 0HE, United Kingdom*

Stavros Athanasopoulos − *Departamento de Física, Universidad Carlos III de Madrid, 28911 Madrid, Spain;* orcid.org/0000-0003-0753-2643

Yun Li − *ARC Centre of Excellence in Exciton Science, School of Chemistry, The University of Sydney, Sydney, New South Wales 2006, Australia*

Samuel N. Sanders − *Department of Chemistry, Columbia University, New York, New York 10027, United States*

Elango Kumarasamy − *Department of Chemistry, Columbia University, New York, New York 10027, United States;* orcid.org/0000-0002-7995-6894

Luis M. Campos − *Department of Chemistry, Columbia University, New York, New York 10027, United States;* orcid.org/0000-0003-2110-2666

Complete contact information is available at: https://pubs.acs.org/10.1021/acs.jpclett.2c02061

Notes

The authors declare no competing financial interest.

■ ACKNOWLEDGMENTS

This work was supported by the Australian Research Council Centre of Excellence in Exciton Science (Grant CE170100026). This work was funded by the Deutsche Forschungsgemeinschaft (DFG, German Research Foundation) − through the project "MARS" (project number 446281755) and was also supported by Comunidad de Madrid (Spain) − multiannual agreement with UC3M ("Excelencia para el Profesorado Universitario" − EPUC3M14) − Fifth regional research plan 2016−2020 and by the Spanish Ministry of Science, Innovation and Universities (MICINN) through project RTI2018-101020-B-100. L.M.C. thanks the National Science Foundation (DMR-2004678). The authors acknowledge the Sydney Informatics Hub and the University of Sydney's high-performance computing cluster Artemis for providing the high-performance computing resources that have contributed to the research results reported in this paper.

■ REFERENCES

(1) Sun, Y.; Welch, G. C.; Leong, W. L.; Takacs, C. J.; Bazan, G. C.; Heeger, A. J. Solution-processed small-molecule solar cells with 6.7% efficiency. *Nat. Mater.* **2012**, *11* (1), 44−48.

(2) Duan, L.; Hou, L.; Lee, T.-W.; Qiao, J.; Zhang, D.; Dong, G.; Wang, L.; Qiu, Y. Solution processable small molecules for organic light-emitting diodes. *J. Mater. Chem.* **2010**, *20* (31), 6392−6407.

(3) Ren, H.; Chen, J.-D.; Li, Y.-Q.; Tang, J.-X. Recent Progress in Organic Photodetectors and their Applications. *Adv. Sci.* **2021**, *8* (1), 2002418.

(4) Ohayon, D.; Inal, S. Organic Bioelectronics: From Functional Materials to Next-Generation Devices and Power Sources. *Adv. Mater.* **2020**, *32* (36), 2001439.
(5) Zafra, J. L.; Molina Ontoria, A.; Mayorga Burrezo, P.; Peña-Alvarez, M.; Samoc, M.; Szeremeta, J.; Ramírez, F. J.; Lovander, M. D.; Droske, C. J.; Pappenfus, T. M.; Echegoyen, L.; López Navarrete, J. T.; Martín, N.; Casado, J. Fingerprints of Through-Bond and Through-Space Exciton and Charge π-Electron Delocalization in Linearly Extended [2.2]Paracyclophanes. *J. Am. Chem. Soc.* **2017**, *139* (8), 3095−3105.
(6) Scholes, G. D.; Ghiggino, K. P.; Oliver, A. M.; Paddon-Row, M. N. Through-space and through-bond effects on exciton interactions in rigidly linked dinaphthyl molecules. *J. Am. Chem. Soc.* **1993**, *115* (10), 4345−4349.
(7) Pasman, P.; Rob, F.; Verhoeven, J. W. Intramolecular charge-transfer absorption and emission resulting from through-bond interaction in bichromophoric molecules. *J. Am. Chem. Soc.* **1982**, *104* (19), 5127−5133.
(8) Paddon-Row, M. N. Some aspects of orbital interactions through bonds: physical and chemical consequences. *Acc. Chem. Res.* **1982**, *15* (8), 245−251.
(9) Walker, B. J.; Musser, A. J.; Beljonne, D.; Friend, R. H. Singlet exciton fission in solution. *Nat. Chem.* **2013**, *5* (12), 1019−1024.
(10) Einzinger, M.; Wu, T.; Kompalla, J. F.; Smith, H. L.; Perkinson, C. F.; Nienhaus, L.; Wieghold, S.; Congreve, D. N.; Kahn, A.; Bawendi, M. G.; Baldo, M. A. Sensitization of silicon by singlet exciton fission in tetracene. *Nature* **2019**, *571* (7763), 90−94.
(11) Rao, A.; Friend, R. H. Harnessing singlet exciton fission to break the Shockley−Queisser limit. *Nat. Mater.* **2017**, *2* (11), 17063.
(12) Smith, M. B.; Michl, J. Recent Advances in Singlet Fission. *Annu. Rev. Phys. Chem.* **2013**, *64* (1), 361−386.
(13) Bera, K.; Kwang, S. Y.; Frontiera, R. R. Advances in Singlet Fission Chromophore Design Enabled by Vibrational Spectroscopies. *J. Phys. Chem. C* **2020**, *124* (46), 25163−25174.
(14) Korovina, N. V.; Pompetti, N. F.; Johnson, J. C. Lessons from intramolecular singlet fission with covalently bound chromophores. *J. Chem. Phys.* **2020**, *152* (4), 040904.
(15) Schnedermann, C.; Alvertis, A. M.; Wende, T.; Lukman, S.; Feng, J.; Schröder, F. A. Y. N.; Turban, D. H. P.; Wu, J.; Hine, N. D. M.; Greenham, N. C.; Chin, A. W.; Rao, A.; Kukura, P.; Musser, A. J. A molecular movie of ultrafast singlet fission. *Nat. Commun.* **2019**, *10* (1), 4207.
(16) Hetzer, C.; Guldi, D. M.; Tykwinski, R. R. Pentacene Dimers as a Critical Tool for the Investigation of Intramolecular Singlet Fission. *Chem. - Eur. J.* **2018**, *24* (33), 8245−8257.
(17) Kumarasamy, E.; Sanders, S. N.; Tayebjee, M. J. Y.; Asadpoordarvish, A.; Hele, T. J. H.; Fuemmeler, E. G.; Pun, A. B.; Yablon, L. M.; Low, J. Z.; Paley, D. W.; Dean, J. C.; Choi, B.; Scholes, G. D.; Steigerwald, M. L.; Ananth, N.; McCamey, D. R.; Sfeir, M. Y.; Campos, L. M. Tuning Singlet Fission in π-Bridge-π Chromophores. *J. Am. Chem. Soc.* **2017**, *139* (36), 12488−12494.
(18) Sanders, S. N.; Kumarasamy, E.; Pun, A. B.; Trinh, M. T.; Choi, B.; Xia, J.; Taffet, E. J.; Low, J. Z.; Miller, J. R.; Roy, X.; Zhu, X. Y.; Steigerwald, M. L.; Sfeir, M. Y.; Campos, L. M. Quantitative Intramolecular Singlet Fission in Bipentacenes. *J. Am. Chem. Soc.* **2015**, *137* (28), 8965−8972.
(19) Basel, B. S.; Hetzer, C.; Zirzlmeier, J.; Thiel, D.; Guldi, R.; Hampel, F.; Kahnt, A.; Clark, T.; Guldi, D. M.; Tykwinski, R. R. Davydov splitting and singlet fission in excitonically coupled pentacene dimers. *Chem. Sci.* **2019**, *10* (13), 3854−3863.
(20) Sakuma, T.; Sakai, H.; Araki, Y.; Mori, T.; Wada, T.; Tkachenko, N. V.; Hasobe, T. Long-Lived Triplet Excited States of Bent-Shaped Pentacene Dimers by Intramolecular Singlet Fission. *J. Phys. Chem. A* **2016**, *120* (11), 1867−1875.
(21) Zirzlmeier, J.; Lehnherr, D.; Coto, P. B.; Chernick, E. T.; Casillas, R.; Basel, B. S.; Thoss, M.; Tykwinski, R. R.; Guldi, D. M. Singlet fission in pentacene dimers. *Proc. Natl. Acad. Sci. U. S. A.* **2015**, *112* (17), 5325−5330.
(22) Krishnapriya, K. C.; Roy, P.; Puttaraju, B.; Salzner, U.; Musser, A. J.; Jain, M.; Dasgupta, J.; Patil, S. Spin density encodes intramolecular singlet exciton fission in pentacene dimers. *Nat. Commun.* **2019**, *10* (1), 33.
(23) Tayebjee, M. J. Y.; Sanders, S. N.; Kumarasamy, E.; Campos, L. M.; Sfeir, M. Y.; McCamey, D. R. Quintet multiexciton dynamics in singlet fission. *Nat. Phys.* **2017**, *13* (2), 182−188.
(24) Sharma, A.; Athanasopoulos, S.; Kumarasamy, E.; Phansa, C.; Asadpoordarvish, A.; Sabatini, R. P.; Pandya, R.; Parenti, K. R.; Sanders, S. N.; McCamey, D. R.; Campos, L. M.; Rao, A.; Tayebjee, M. J. Y.; Lakhwani, G. Pentacene−Bridge Interactions in an Axially Chiral Binaphthyl Pentacene Dimer. *J. Phys. Chem. A* **2021**, *125* (33), 7226−7234.
(25) Kobayashi, N.; Nakai, K. Applications of magnetic circular dichroism spectroscopy to porphyrins and phthalocyanines. *Chem. Commun.* **2007**, *40*, 4077−4092.
(26) Stephens, P. J. Magnetic Circular Dichroism. *Annu. Rev. Phys. Chem.* **1974**, *25* (1), 201−232.
(27) Kuno, M.; Nirmal, M.; Bawendi, M. G.; Efros, A.; Rosen, M. Magnetic circular dichroism study of CdSe quantum dots. *J. Chem. Phys.* **1998**, *108* (10), 4242−4247.
(28) Pandya, R.; Steinmetz, V.; Puttisong, Y.; Dufour, M.; Chen, W. M.; Chen, R. Y. S.; Barisien, T.; Sharma, A.; Lakhwani, G.; Mitioglu, A.; Christianen, P. C. M.; Legrand, L.; Bernardot, F.; Testelin, C.; Chin, A. W.; Ithurria, S.; Chamarro, M.; Rao, A. Fine Structure and Spin Dynamics of Linearly Polarized Indirect Excitons in Two-Dimensional CdSe/CdTe Colloidal Heterostructures. *ACS Nano* **2019**, *13* (9), 10140−10153.
(29) Henning, G. N.; McCaffery, A. J.; Schatz, P. N.; Stephens, P. J. Magnetic Circular Dichroism of Charge-Transfer Transitions: Low-Spin d5 Hexahalide Complexes. *J. Chem. Phys.* **1968**, *48* (12), 5656−5661.
(30) Michl, J. Magnetic circular dichroism of cyclic.pi.-electron systems. 1. Algebraic solution of the perimeter model for the A and B terms of high-symmetry systems with a (4N + 2)-electron [n]annulene perimeter. *J. Am. Chem. Soc.* **1978**, *100* (22), 6801−6811.
(31) Michl, J. Magnetic circular dichroism of cyclic.pi.-electron systems. 3. Classification of cyclic.pi. chromophores with a (4N + 2)-electron [n]annulene perimeter and general rules for substituent effects on the MCD spectra of soft chromophores. *J. Am. Chem. Soc.* **1978**, *100* (22), 6819−6824.
(32) Michl, J. Magnetic circular dichroism of cyclic.pi.-electron systems. 2. Algebraic solution of the perimeter model for the B terms of systems with a (4N + 2)-electron [n]annulene perimeter. *J. Am. Chem. Soc.* **1978**, *100* (22), 6812−6818.
(33) Ghidinelli, S.; Longhi, G.; Abbate, S.; Hättig, C.; Coriani, S. Magnetic Circular Dichroism of Naphthalene Derivatives: A Coupled Cluster Singles and Approximate Doubles and Time-Dependent Density Functional Theory Study. *J. Phys. Chem. A* **2021**, *125* (1), 243−250.
(34) Kaminský, J.; Chalupský, J.; Štěpánek, P.; Kříž, J.; Bouř, P. Vibrational Structure in Magnetic Circular Dichroism Spectra of Polycyclic Aromatic Hydrocarbons. *J. Phys. Chem. A* **2017**, *121* (47), 9064−9073.
(35) Toriumi, N.; Muranaka, A.; Kayahara, E.; Yamago, S.; Uchiyama, M. In-Plane Aromaticity in Cycloparaphenylene Dications: A Magnetic Circular Dichroism and Theoretical Study. *J. Am. Chem. Soc.* **2015**, *137* (1), 82−85.
(36) Gorski, A.; Kijak, M.; Zenkevich, E.; Knyukshto, V.; Starukhin, A.; Semeikin, A.; Lyubimova, T.; Roliński, T.; Waluk, J. Magnetic Circular Dichroism of meso-Phenyl-Substituted Pd-Octaethylporphyrins. *J. Phys. Chem. A* **2020**, *124* (40), 8144−8158.
(37) Meskers, S. C. J.; Polonski, T.; Dekkers, H. P. J. M. Polarized Absorption and Phosphorescence Spectra and Magnetic Circular Dichroism of Dithioimides: Assignment of the Lower 1n.pi. and 3n.pi. States. *J. Phys. Chem.* **1995**, *99* (4), 1134−1142.
(38) Hughes, J. L.; Razeghifard, R.; Logue, M.; Oakley, A.; Wydrzynski, T.; Krausz, E. Magneto-Optic Spectroscopy of a Protein

https://doi.org/10.1021/acs.jpclett.2c02061
J. Phys. Chem. Lett. 2022, 13, 8978−8986

Tetramer Binding Two Exciton-Coupled Chlorophylls. *J. Am. Chem. Soc.* **2006**, *128* (11), 3649−3658.
(39) Umetsu, M.; Seki, R.; Wang, Z.-Y.; Kumagai, I.; Nozawa, T. Circular and Magnetic Circular Dichroism Studies of Bacteriochlorophyll c Aggregates: T-Shaped and Antiparallel Dimers. *J. Phys. Chem. B* **2002**, *106* (15), 3987−3995.
(40) Houssier, C.; Sauer, K. Circular dichroism and magnetic circular dichroism of the chlorophyll and protochlorophyll pigments. *J. Am. Chem. Soc.* **1970**, *92* (4), 779−791.
(41) Sharma, A.; Wojciechowski, J. P.; Liu, Y.; Pelras, T.; Wallace, C. M.; Müllner, M.; Widmer-Cooper, A.; Thordarson, P.; Lakhwani, G. The Role of Fiber Agglomeration in Formation of Perylene-Based Fiber Networks. *Cell. Rep. Phys. Sci.* **2020**, *1* (8), 100148.
(42) Chapter 10 Michl's Perimeter Model in MCD Spectroscopy. In *Circular Dichroism and Magnetic Circular Dichroism Spectroscopy for Organic Chemists*; The Royal Society of Chemistry, 2012; pp 172−191.
(43) Kobayashi, M.; Wang, Z.-Y.; Yoza, K.; Umetsu, M.; Konami, H.; Mimuro, M.; Nozawa, T. Molecular structures and optical properties of aggregated forms of chlorophylls analyzed by means of magnetic circular dichroism. *Spectrochim. Acta A Mol. Biomol. Spectrosc.* **1996**, *52* (5), 585−598.
(44) Parenti, K. R.; He, G.; Sanders, S. N.; Pun, A. B.; Kumarasamy, E.; Sfeir, M. Y.; Campos, L. M. Bridge Resonance Effects in Singlet Fission. *J. Phys. Chem. A* **2020**, *124* (45), 9392−9399.
(45) McConnell, H. M. Intramolecular Charge Transfer in Aromatic Free Radicals. *J. Chem. Phys.* **1961**, *35* (2), 508−515.
(46) Klevens, H. B.; Platt, J. R. Spectral Resemblances of Cata-Condensed Hydrocarbons. *J. Chem. Phys.* **1949**, *17* (5), 470−481.
(47) Mondal, R.; Tönshoff, C.; Khon, D.; Neckers, D. C.; Bettinger, H. F. Synthesis, Stability, and Photochemistry of Pentacene, Hexacene, and Heptacene: A Matrix Isolation Study. *J. Am. Chem. Soc.* **2009**, *131* (40), 14281−14289.
(48) Hele, T. J. H.; Fuemmeler, E. G.; Sanders, S. N.; Kumarasamy, E.; Sfeir, M. Y.; Campos, L. M.; Ananth, N. Anticipating Acene-Based Chromophore Spectra with Molecular Orbital Arguments. *J. Phys. Chem. A* **2019**, *123* (13), 2527−2536.
(49) Steiner, R. P.; Michl, J. Magnetic circular dichroism of cyclic.pi.-electron systems. 11. Derivatives and aza analogues of anthracene. *J. Am. Chem. Soc.* **1978**, *100* (22), 6861−6867.
(50) Jones, A. O. F.; Chattopadhyay, B.; Geerts, Y. H.; Resel, R. Substrate-Induced and Thin-Film Phases: Polymorphism of Organic Materials on Surfaces. *Adv. Funct. Mater.* **2016**, *26* (14), 2233−2255.
(51) Hughes, J. L.; Pace, R. J.; Krausz, E. The exciton contribution to the Faraday B term MCD of molecular dimers. *Chem. Phys. Lett.* **2004**, *385* (1), 116−121.
(52) Jordan, K. D.; Paddon-Row, M. N. Analysis of the interactions responsible for long-range through-bond-mediated electronic coupling between remote chromophores attached to rigid polynorbornyl bridges. *Chem. Rev.* **1992**, *92* (3), 395−410.
(53) Ito, S.; Nagami, T.; Nakano, M. Design Principles of Electronic Couplings for Intramolecular Singlet Fission in Covalently-Linked Systems. *J. Phys. Chem. A* **2016**, *120* (31), 6236−6241.
(54) Ito, S.; Nagami, T.; Nakano, M. Rational design of doubly-bridged chromophores for singlet fission and triplet−triplet annihilation. *RSC Adv.* **2017**, *7* (55), 34830−34845.

https://doi.org/10.1021/acs.jpclett.2c02061
J. Phys. Chem. Lett. 2022, 13, 8978−8986